

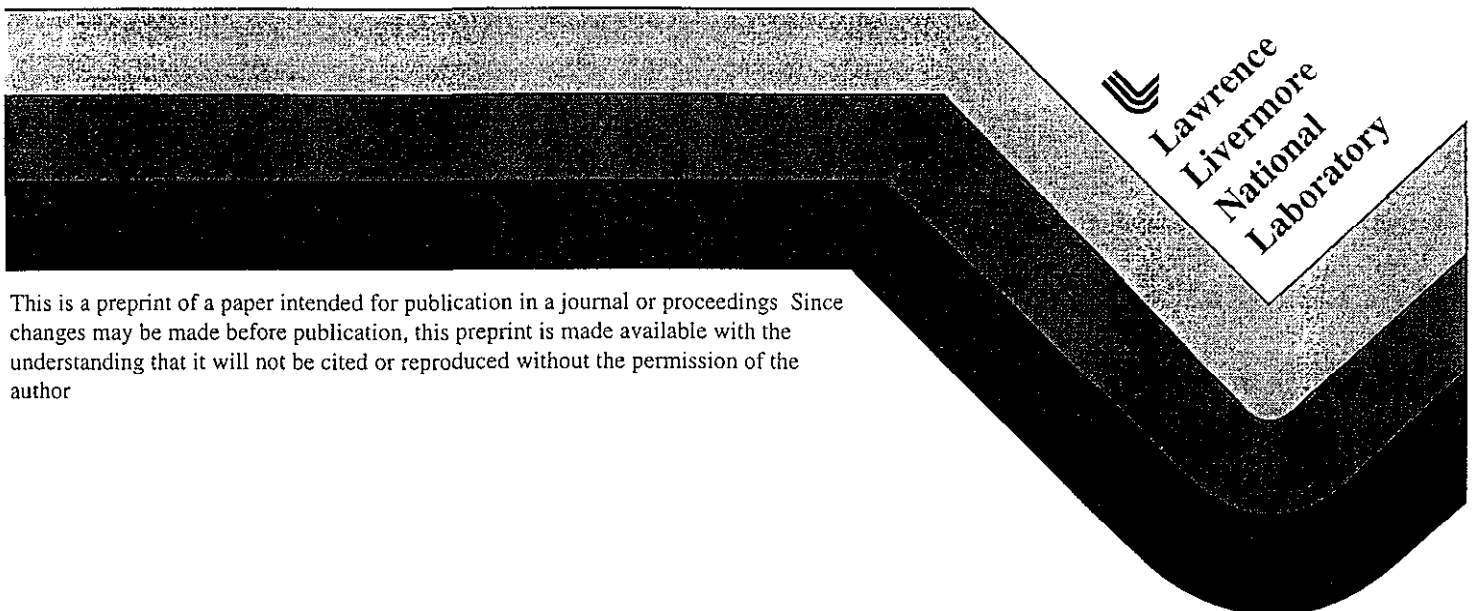
UCRL-JC-127554
PREPRINT

Kinetic Information from Detonation Front Curvature

P C Souers
R Garza

This paper was prepared for submittal to the
Eleventh International Detonation (1998) Symposium
Snowmass, CO
Aug 31- Sept 4, 1998

June 15, 1998



This is a preprint of a paper intended for publication in a journal or proceedings. Since changes may be made before publication, this preprint is made available with the understanding that it will not be cited or reproduced without the permission of the author.

DISCLAIMER

This document was prepared as an account of work sponsored by an agency of the United States Government. Neither the United States Government nor the University of California nor any of their employees, makes any warranty, express or implied, or assumes any legal liability or responsibility for the accuracy, completeness, or usefulness of any information, apparatus, product, or process disclosed, or represents that its use would not infringe privately owned rights. Reference herein to any specific commercial product, process, or service by trade name, trademark, manufacturer, or otherwise, does not necessarily constitute or imply its endorsement, recommendation, or favoring by the United States Government or the University of California. The views and opinions of authors expressed herein do not necessarily state or reflect those of the United States Government or the University of California, and shall not be used for advertising or product endorsement purposes.

KINETIC INFORMATION FROM DETONATION FRONT CURVATURE

P. Clark Souers and Raul Garza

Energetic Materials Center, Lawrence Livermore National Laboratory, Livermore, California 94550 (USA)

The time constants for time-dependent modeling may be estimated from reaction zone lengths, which are obtained from two sources. One is detonation front curvature, where the edge lag is close to being a direct measure. The other is the Size Effect, where the detonation velocity decreases with decreasing radius as energy is lost to the cylinder edge. A simple theory that interlocks the two effects is given. A differential equation for energy flow in the front is used, the front is described by quadratic and sixth-power radius terms. The quadratic curvature comes from a constant power source of energy moving sideways to the walls. Near the walls, this energy rises to the total energy of detonation and produces the sixth-power term. The presence of defects acting on a short reaction zone can eliminate the quadratic part while leaving the wall portion of the curvature. A collection of TNT data shows that the reaction zone increases with both the radius and the void fraction.

QUADRATIC CURVATURES

New kinetic, i.e. time-dependent, explosive models need input data, and a first cut may be had by obtaining reaction zone lengths for promptly detonating explosives at steady state, i.e. with constant two-dimensional confinement effects. Direct measurements of these reaction zones have not been made, so that any approach will necessarily be indirect.

Detonation front curvatures of cylinders offer a starting point, and most measured curvatures are of the "quadratic" type as illustrated by J. Lee's ANFO data in Figure 1¹. The curves are smooth, roughly quadratic and

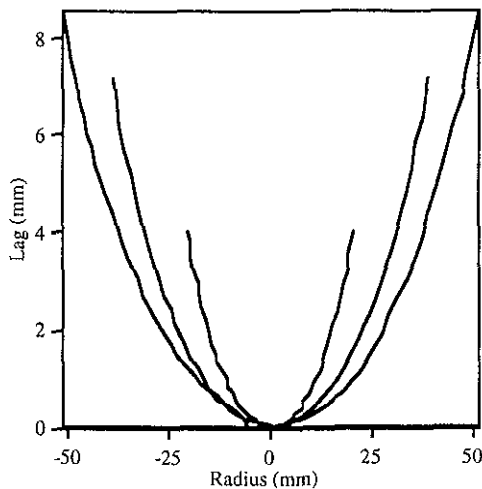


FIGURE 1 Three radii of unconfined ANFO cylinders fires by J. Lee. These are of the smooth "quadratic" type. The detonation is proceeding downward.

show an edge lag that increases with increasing radius. The curves are not truly quadratic but may be described by the function²

$$L = AR^2 + BR^6 \quad (1)$$

where L is the detonation lag and R is the radius. A and B are constants for a given radius but are variable for different radii. The A -term may be thought of as describing the continuous flow of energy from the cylinder axis outward to support the edges. The B -term represents the break-out of the wall and shows more scatter in the fitted data. The A -term contributes about 50% of the edge lag for small reaction-zone explosives and perhaps 70% for large ones, with there being wide scatter. The "average" position for Eq. 1 occurs at about $R_0/2^{1/2}$.

Figure 2 shows a schematic of the reaction zones, both sonic and percent chemical reaction. The explosive tries to minimize both the lag and the sonic reaction zone, which suggests the approximation that²

$$\langle x_c \rangle \sim L_0 \quad (2)$$

where $\langle x_c \rangle$ is the average sonic reaction zone length and

L_0 the edge lag.

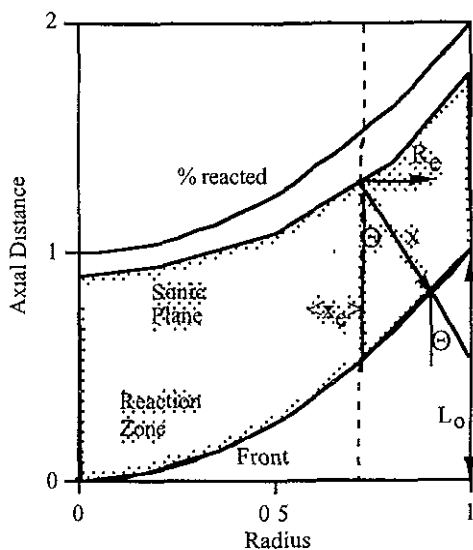


FIGURE 2 Schematic view of the sonic reaction zone for a "quadratic" curvature Θ is the angle of the front at radius R , $\langle x_e \rangle$ is the average sonic reaction zone length A chemical reaction zone is also shown Detonation is downward

The angle normal to the front at radius R is given by the derivative

$$\Theta = \tan^{-1}(2AR + 6BR^5) \quad (3)$$

One test of Eq 3 is the measurement of the edge angle at R_0 , which will be 0° for a flat front and larger as the curvature increases Table 1 lists the measured and calculated edge angles taken only from high quality runs where digital files are available³⁻⁷ The radius of curvature, which varies with radius, is

$$R_{cur} = R/\sin\Theta \quad (4)$$

Considerable error exists in determining the experimental angles The various families of explosives show the same measured edge angle within error The addition of metal containment, seen with the PBXN-111, reduces both the lag and the angle An exceptionally large angle appears in the PBX-9502 data

TABLE 1 Measured and calculated edge angles for assorted explosives PETN and LX-14 are not quadratic

	Degrees		Measd Stdev
	Meas	Calc	
PETN	3	3	
LX-14	4	5	
QM100R	12	9	5
LX-04	14	9	9
PBXN-111- N Con	16	16	8
PBXN-111- A Con	17	15	7
Ultrafine TATB	18	14	3
NM ANFO	20	26	5
PBXN-111-N Unc	26	30	10
HANFO	26	36	11
PBXN-111-A Unc	33	31	18
PBX-9502	39	22	16

The Size Effect theory for a cylinder was constructed with the relations⁸

$$\begin{aligned} \left(\frac{\langle E_0 \rangle}{E_0} \right)^{1/2} &= \frac{U_s}{D} = 1 - \frac{R_e}{R_0} \\ &= 1 - \frac{\langle x_e \rangle}{\sigma R_0} \end{aligned} \quad (5)$$

where $\langle E_0 \rangle$ and U_s , E_0 and D are the total detonation energies and velocities in cylinders of radius R_0 and infinite size, respectively "Infinite" radius also means radius R_0 with perfect wall confinement R_e is the thickness of the skin layer on the edge that loses all energy and requires energy replacement from the interior σ is a function that relates R_e and the reaction zone length Eq 5 is a relation between cylindrical volumes, chemical energy density and detonation velocity

It would be useful to relate curvature with the Size Effect, where the detonation velocity changes with radius In Figure 2, at the average radius $\langle R \rangle = 0.707R_0$, we define the average angle of the front $\langle \Theta \rangle$ and write

$$\langle x_e \rangle \approx \frac{R_o(1 - U_s/D)}{\sin\langle\theta\rangle\cos\langle\Theta\rangle} \quad (6)$$

where we assume that the sideways distance for energy to be shipped is equal to the skin layer thickness, R_c

From Eqs 5 and 6, we see that

$$\sigma = [\sin\langle\Theta\rangle\cos\langle\Theta\rangle]^{-1} \quad (7)$$

The result of this approach is that the equality of reaction zone length and edge lag given in Eq 2 is only approximately true. We find, for the TATB, PBXN-111 and ANFO groups, an average ratio of

$$\langle x_e \rangle / L_o \sim 2.3 \pm 1.6 \quad (8)$$

SIMPLE DERIVATION

The "quadratic" shape arises because the explosive moves energy sideways to shore up the moving wall. We use the mathematics for calculation of temperature in a cylinder with internal heat generation.⁹ The lag, L , may be described by^{2,8}

$$\nabla^2 L = \frac{1}{R} \frac{\partial}{\partial R} \left(R \frac{\partial L}{\partial R} \right) = \frac{A_o}{K} = 4A + 36BR^4 \quad (9)$$

where R is the radius, A_o is the sideways power and K is the energy conductivity

We can calculate the A term by assuming that all of the constant sideways quadratic energy is given by $E_o - \langle E_o \rangle$, which, from Eq 5, is

$$\begin{aligned} E_o - \langle E_o \rangle &= \beta \left[1 - \left(1 - \frac{\langle x_e \rangle}{\sigma R_o} \right)^2 \right] E_o \\ &\approx \frac{2\beta \langle x_e \rangle E_o}{\sigma R_o} \end{aligned} \quad (10)$$

Above, βE_o is the total actual energy of detonation obtained within the reaction zone, so that E_o is reserved for the total energy calculated from the thermochemical code. For most homogeneous and heterogeneous explosives, we expect β to be 1, but for composites, it may be much smaller. For PBXN-111, for example, the aluminum and AP probably do not react within the reaction zone, so that $\beta E_o \approx 2-4$ kJ/cc whereas the complete reaction produces 13 kJ/cc

The power in Eq 9 is the energy divided by time, which is $1/U_s$ across 1 cm. We divide by K and compare with 4A from Eq 9

$$A = \left(\beta \frac{U_s E_o}{K} \right) \frac{\langle x_e \rangle}{2\sigma R_o} \quad (11)$$

A is obtained from the curvature, so that we get the energy conductivity from

$$K = \frac{\beta E_o U_s}{A} \left(\frac{\langle x_e \rangle}{2\sigma R_o} \right) \quad (12)$$

For TATB explosives, $K \sim 90 \pm 50$ MW/mm². For PBXN-111 and ANFO $K \sim 90 \pm 4$ and 300 ± 220 MW/mm²

Overall, K is roughly 100 MW/mm². We have no similar treatment for B

The energy density of an imaginary 1 cc cube may be converted to total energy, differentiated and adjusted for the side surface area to give the pressure on the front

$$\begin{aligned} P &= P_o - \frac{K}{U_s} (4A + 36BR^4) \\ &= P_{\max} - \frac{K}{U_s} 36BR^4 \end{aligned} \quad (13)$$

The pressure is expected to decrease more steeply than the curvature increased. For TATB explosives, we find the maximum B term to amount to 0 GPa for $R_o = 25$ mm but 4-11 GPa for $R_o = 5-6$ mm

For the Wood-Kirkwood 1/2-dimensional analytical model that describes a single cell on the axis of a cylinder,¹⁰ we define a radius of curvature of the detonation front

$$R_{cur} \sim R/(2AR + 6BR^5) \rightarrow 1/2A \text{ for } R \rightarrow \infty \quad (14)$$

Using the equations above, the radial particle velocity in the model is

$$u_r = \frac{P \tan \Theta}{\rho_o U_s} = \frac{1}{\rho_o U_s} \left(P_o - \frac{K}{U_s} 4A - \frac{K}{U_s} 36BR^4 (2AR + 6BR^5) \right) \quad (15)$$

and the radial W-K function becomes

$$\begin{aligned} \frac{\partial u_r}{\partial R} = \omega_r &= \frac{2A}{\rho_o U_s} \left(P_o - \frac{K}{U_s} 4A \right) \\ &= \frac{2AP(\text{axis})}{\rho_o U_s} = \frac{u_p}{R_{cur}} \end{aligned} \quad (16)$$

It would be useful to obtain an on-axis radius of curvature from the Size Effect data. Using Eq 7, we can calculate from σ to $\langle \Theta \rangle$ by iteration. Unfortunately, $\langle \Theta \rangle$ contains elements of B as well as A, so that on-axis behavior for curvatures is given to $\pm 15\%$ by

$$R_{cur}(\text{on-axis}) = \frac{1}{2A} \approx \frac{R_o}{\tan \langle \Theta \rangle} \quad (17)$$

This is used to calculate R_{cur} from the Size Effect data

NON-QUADRATIC CURVES

A second type of non-quadratic curvature is found for explosives with small reaction zones, as seen for 1.82 g/cc LX-14 (95.5% HMX, 4.5% estane) in Figure 3.³ The center is ragged and turbulent and often contains a "sombbrero" perhaps caused by non-parallel cylinder faces. Excluding the center, the curve may be fit to

$$L = BR^6 \quad (18)$$

so that only the wall term is present. We postulate that defects such as inert grains or large voids scatter the front, and only the energy from the outermost regions flows to the edges. The curve is symmetric because the defect size

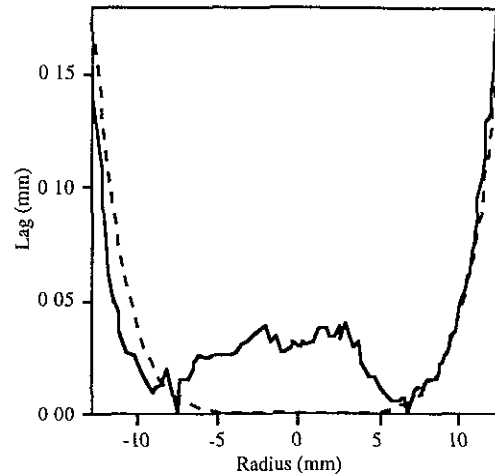


FIGURE 3 Detonation front curvature of non-quadratic LX-14 taken with a 7500 rpm rotor and a writing speed of 30 mm/ μ s. The dashed line fits BR^6 . A tilt correction to the data has been made.

is much smaller than the cylinder radius.

Another non-quadratic case appears when the defect size is about 1/10 the radius and extreme disruption of the front occurs. Figure 4 shows two shots with the paste explosive RX-08-HD (74% HMX, 20 TMETN, 6 urethane binder).³ The upper one is defect-free and shows a quadratic shape. The lower had mm-sized holes as seen by x-rays. The center is massively disrupted, yet the edge lags are still visible: 1.1 mm for the top and 0.4 - 0.6 mm at the bottom, suggesting that the holes cut the reaction zone length in half. The detonation velocities were 8.15 and 8.04 mm/ μ s, showing that the defects do indeed slow the speed.

THE SIZE EFFECT

We return to further consider the Size Effect and see if we can get more data to use. We use Eq 7 to calculate σ for the curvature samples with TATB, PBXN-111, ANFO

and other individual samples where D can be extrapolated with some confidence. The results are plotted in Figure 5 vs $1 - U_s/D$ and the fitted curve is

$$\sigma \approx \frac{2.2}{(1 - U_s/D)^{1/3}} \quad (19)$$

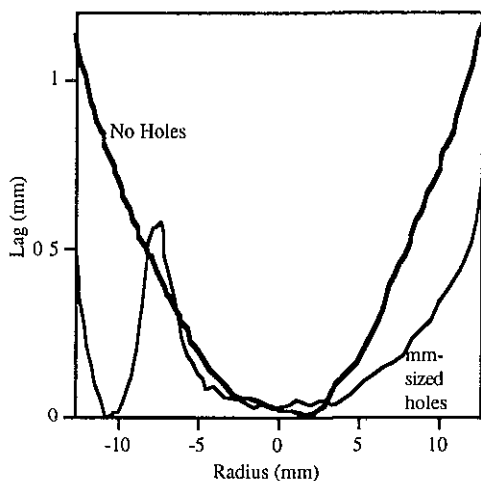


FIGURE 4 Effects of holes in distorting the detonation front of the paste explosive RX-08-HD

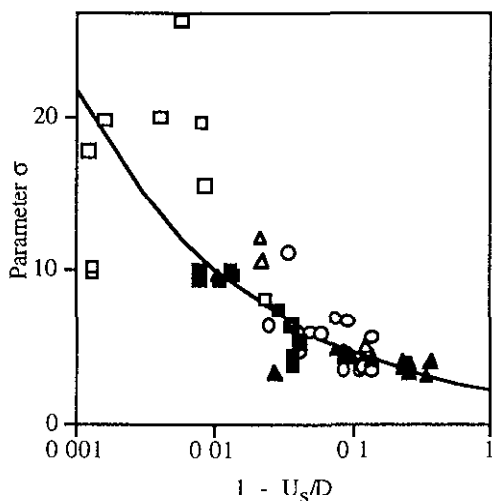


FIGURE 5 Calibrating the σ function with curvature data. The data includes all types of explosives where D can be reasonably extrapolated

Using this, we may take all the Size Effect data that exists and calculate the Size Effect reaction zone lengths from Eq. 5

$$\langle x_e \rangle = \sigma R_o \left(1 - \frac{U_s}{D} \right) \quad (20)$$

CONVERTING TO KINETICS

We next want to convert our results to obtain the time constant, τ , where the simplest burn relation might be

$$\frac{dF}{dt} = G \frac{P^2(1-F)}{\tau} \quad (21)$$

where F is the fraction burned, P the pressure and G the rate constant. The best that we can do is assume the same number of time constants, $n \sim 5$, in the burn of every explosive. Many (but not all) samples follow this empirical relation

$$\langle x_e \rangle / R_o^{1/2} \sim \text{constant} \quad (22)$$

This allows us to calculate $\langle x_e \rangle$ for a constant set of radii, a possibly unnecessary refinement. The rate constant for Eq. 21 is roughly

$$G \approx \frac{5U_s}{\langle x_e \rangle (5P_{CJ}/4)^2} \quad (23)$$

where the thermochemical C-J pressure is multiplied by 5/4 to approximate the spike pressure. Table 2 shows a comparative list of rate constants that might be used as input to a kinetic code.

DISCUSSION

The reaction zone lengths have been derived using a circular model and are good to perhaps $\pm 100\%$. Only direct measurement with gauges will fix the numbers, and we might expect them to all move in proportion. We next consider the broad TNT data set of Stesik and Akimova ¹¹

TABLE 2 Table of comparative rates obtained from Size Effect data for a 12.7 mm radius. Five time constants inside the reaction length are used.

	$\langle x_e \rangle$ (mm)	G (μs^{-1} *) (GPa^{-2})
TNT 1.62 g/cc	1.4	0.04
PBX-9404	0.6	0.04
TNT 1.0 g/cc	6.5	0.045
PBX-9501	0.6	0.04
Comp B	0.9	0.04
ANFO SW	8	0.02
ANFO 0.95 g/cc	11	0.022
PBX-9502	2.3	0.014

Figure 6 shows the calculated ratio $\langle x_e \rangle / R_0^{1/2}$ plotted as a function of void volume, f_v , for cylinders of various radii. The void volume is calculated from

$$f_v = 1 - \rho_0 / \rho(TMD) \quad (24)$$

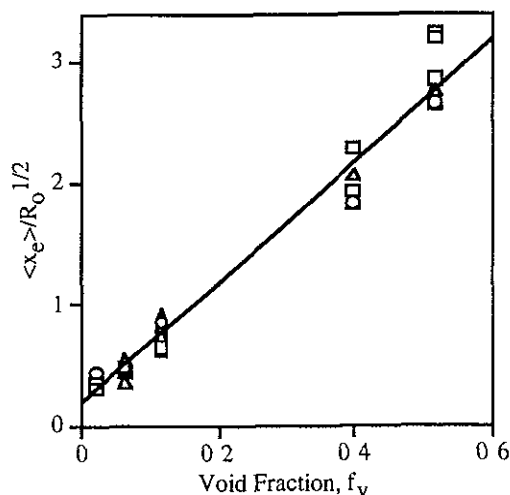


FIGURE 6. Reaction zone length for cylinders of fixed radius for TNT.¹³ Void space increases the reaction zone. The circles are 15-16 mm radii, squares are for 4-5 mm, the rest from 1.6-20 mm are triangles

The data in Figure 6 may be fit by the empirical equation

$$\langle x_e \rangle / R_0^{1/2} \sim 0.18 + 5.0 f_v \quad (25)$$

The $R_0^{1/2}$ term removes the dependence of the radius for these samples. The reaction zone increases with increasing void fraction but by much more than might be expected. If only the void volume were added directly to the reaction zone volume, we would expect

$$\langle x_e \rangle / R_0^{1/2} \sim 0.18 + 0.36 f_v \quad (26)$$

Does the approach of Eq. 25 work for the other Size Effect data? The results are shown in Figure 7. The fast group of explosives includes PETN, RDX, HMX, ADNBF, DNBF and "pure" TNT. Some explosives with a few percent binder are included. The slow group includes "impure TNT" (Figure 6), tetryl, DNT, EDNA, picric acid, TATB, NTO, DINGU and RDX/polyethylene wax. The general appearance of the figure is the same

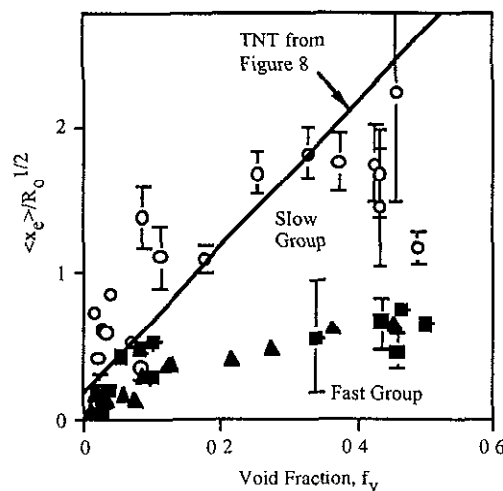


FIGURE 7. Addition of more Size Effect data to the TNT line of Figure 6. A slow and a fast group of explosives are defined.

SUMMARY DATA

A collection of detonation front curvature and Size Effect data is available in P. C. Souers, "A Library of Prompt Detonation Reaction Zone Data," Lawrence Livermore Laboratory UCRL-ID-130055 (1998).

ACKNOWLEDGEMENTS

We wish to thank Jerry Forbes, Per-Anders Persson, John Bdzil, Finn Ouchterlony and David Kennedy for their kind

assistance in supplying curvature data from their laboratories. This work was performed under the auspices of the U S Department of Energy by the Lawrence Livermore National Laboratory under contract number W-7405-ENG-48

REFERENCES

- 1 Jaimin Lee, *Detonation Shock Dynamics of Composite Energetic Materials*, PhD Thesis, New Mexico Institute of Mining and Technology, Socorro, New Mexico, 1990. Per-Anders Persson kindly lent us a copy of the thesis
- 2 P C Souers and R Garza, "Detonation Front Curvature and the Size Effect," *American Physical Society Topical Conference on Shock Compression, Amherst, MA, July 26-August 1, 1997*
- 3 LLNL Cylinder Test
- 4 J W Forbes, E R Lemar, G T Sutherland and R N Baker, Detonation Wave Curvature, *Corner Turning and Unreacted Hugoniot of PBXN-111*, Naval Surface Warfare

Center Report NSWCDD/TR-92/164, Silver Spring, MD, 1992

- 5 J W Forbes, LLNL, private communication, 1997
- 6 David Kennedy, ICI Australia Operations, Kurri Kurri, New South Wales, Australia, private communications, 1995-1997
- 7 John Bdzil, Los Alamos National Laboratory, Los Alamos, NM, private communication, 1996
- 8 P C Souers, "Size Effect and Detonation Front Curvature," *Propellants, Explosives, Pyrotechnics*, 22, 221-225 (1997)
- 9 H S Carslaw and J C Jaeger, *Conduction of Heat in Solids*, 2nd ed (Clarendon Press, Oxford, 1959), pp 130-132, 191, 232
- 10 W W Wood and J G Kirkwood, "Diameter Effect in Condensed Explosives. The Relation between Velocity and Radius of Curvature of the detonation Wave," *J Chem Phys* 22, 1920-1924 (1954)
- 11 L N Stesik and L N Akimova, "An Indirect Method of Estimating the Reaction Zone Width of a Detonation Wave," *Russ J Phys Chem*, 33, 148-151 (1959)

Technical Information Department • Lawrence Livermore National Laboratory
University of California • Livermore, California 94551

